Dynamics of laser-produced Sn microplasma for a high-brightness extreme ultraviolet light source

S. Yuspeh,[a] Y. Tao, R. A. Burdt, M. S. Tillack, Y. Ueno, and F. Najmabadi
Department of Electrical and Computer Engineering and Center for Energy Research, University of California–San Diego, 9500 Gilman Drive, La Jolla, California 92093-0438, USA

(Received 31 January 2011; accepted 19 April 2011; published online 18 May 2011)

The effect of laser focal spot diameters of 26 and 150 μm on 13.5 nm extreme ultraviolet (EUV) radiation is investigated. Simulations show that the smaller spot size has a shorter electron plasma density scale length and deeper and denser laser energy deposition region. This results in additional time required for plasma expansion and radiation transport to efficiently emit EUV light. This is experimentally observed as an increase in the delay between the EUV emission and the laser pulse. The shorter scale length plasma reabsorbs less EUV light, resulting in a higher conversion efficiency, smaller and slightly brighter light source. © *2011 American Institute of Physics*. [doi:10.1063/1.3589359]

The development of Sn laser-produced plasmas (LPPs) has almost exclusively focused on production of 13.5 nm extreme ultraviolet (EUV) light for next generation high volume manufacturing (HVM) lithography of semiconductor microchips with feature size of 22 nm and below. However, there is a growing concern about the ability to detect defects in the multilayer Mo/Si dielectric reflective optics used as mirrors and masks in such systems.[1] Mo/Si mirrors in the system used for HVM will efficiently reflect (70% per mirror) 13.5 nm light [2% bandwidth (BW)].[2] Only actinic (in-band 13.5 nm) light can penetrate deep into the multiple layers to detect defects embedded between layers known as phase defects.[3] Currently, metrology work has been performed using EUV light generated by synchrotron radiation but this is too costly for production purposes.[4,5]

The ideal light source is dramatically different for the HVM and metrology applications. The HVM EUV light source is excessive in terms of power, cost, and size (footprint). An HVM lithography source needs to have at least 115 W at intermediate focus, lifetime of 30 000 h, etendue of less than 3.3 mm^2 sr and high conversion efficiency (CE), laser to in-band 13.5 nm EUV light in a solid angle of 2π sr.[6] To keep the cost of ownership low, the CE is a key figure of merit for HVM light sources as the laser is one of the most expensive components. While the specifications of an actinic metrology light source have not yet converged to specific requirements, the light source needs to be stable, small (etendue on the order of 0.03 mm^2 sr), and bright (several watts of power). This means that the focal spot size and laser energy of the metrology source are much smaller than a HVM lithography source, potentially on the order of 30 μm and several millijoules per pulse.

Due to the size requirements of the laser spot and plasma size for a metrology source, a 1.064 neodymium-doped yttrium aluminum garnet (Nd:YAG) laser is a better option than the 10.6 μm CO_2 laser that is used for HVM lithography, which has been shown to produce higher CE.[7] Whereas there have been several studies showing spot size dramatically affects the plasma at both laser wavelengths,[8,9] very little work has been conducted with spots sizes on the order of 30 μm, especially with pure Sn. Hou *et al.*[10] produced CE around 2% using a 30 μm spot size with Sn doped water droplets, however, the focus was on the design of the fiber laser used and not the plasma. Also, there has been work conducted using relatively small focal spot sizes with various materials, both solid targets and puff gas targets, for probing and surface metrology at other soft x-ray and water window wavelengths.[11,12] In this report, we investigate the different plasma dynamics of HVM (150 μm spot size) and metrology (26 μm spot size) Nd:YAG Sn LPP at the same laser intensity, both experimentally and numerically. Additionally, we establish a baseline in to which further improvements could be made to a Sn LPP EUV metrology light source.

The experimental setup for the HVM source has been previously described.[13] A similar setup was used for the metrology source except for minor modifications due to the low intensity and small scale of the metrology source. A 7 ns full width half maximum (FWHM) Nd:YAG laser was focused to spot sizes of 26 μm and 150 μm ($1/e^2$) with a laser intensity of 2×10^{11} W/cm^2, corresponding to energies of 7.6 mJ and 250 mJ, respectively. The targets irradiated were glass slides and spheres, both coated with 2–3 μm of high purity Sn. Sphere diameters of 50 and 290 μm were used to maintain the same sphere diameter to focal spot size ratio.[14] A 130 ps Nd:YAG laser operating at 532 nm propagating in the focal plane was used as a probe beam in a Nomarski interferometer.

An absolutely calibrated EUV energy monitor (E-Mon) (from Jenoptik) was positioned at 39° from target normal for the HVM experiment. The low energy of the metrology source was below the E-Mon sensitivity. However, the combination of a single Mo/Si multilayer mirror along with a filter pinhole x-ray diode (XRD) (International Radiation Detectors AXUV-HS5) was used for time-resolved EUV emission and calibrated from the E-Mon to calculate the CE of the metrology source. The combination of a single Mo/Si mirror and XRD records 13.5 nm (4% BW) EUV light. The angular distribution measured by Sequoia *et al.*[15] was assumed for all CE calculations. Simultaneously, a fast photodiode (Electro-Optics Technology ET-2000) recorded the temporal profile of the laser pulse.

A concave Mo/Si mirror focused light through a Zr filter onto a back illuminated x-ray charge coupled device (CCD)

[a]Electronic mail: syuspeh@ucsd.edu.

TABLE I. CE and plasma scale lengths for difference focal spot size and target geometry combinations.

Focal spot size ($1/e^2$) (μm)	Target	CE (%)	Scale length (l_s) (μm)
26	Planar	2.5 ± 0.1	46
	Sphere	2.4 ± 0.2	42
150	Planar	1.33 ± 0.02	165
	Sphere	1.4 ± 0.1	115

camera (Princeton Instruments Pi-SX) and recorded the time-integrated 13.5 nm (4% BW) EUV spatial emission. For the HVM source experiment an identical setup to previous experiments was used, having a 5× system magnification and spatial resolution better than 5 μm.[13] Modifications were made to the metrology time-integrated EUV imaging system to increase the magnification to 9× with better than 3 μm spatial resolution.

Numerical simulations of the spherical target experiments were carried out using h2d,[16] a two-dimensional (2D) radiation-hydrodynamic code in Lagrangian coordinates, under the same operating parameters of previously benchmarked work.[13]

The CE for planar and spherical targets for both focal spot sizes are shown in Table I. One of the main reasons for the metrology LPPs having higher CEs are differences in their electron density profile. The density profile plays a key role in the generation and transport of the in-band EUV light due to reabsorption of EUV by the plasma itself.[15,17] Electron density profile maps at the peak of the laser pulse for a HVM plasma and a metrology plasma are shown in Figs. 1(a) and 1(b), respectively, using both planar (top half) and spherical (bottom half) targets with the corresponding electron plasma density scale lengths (l_s) shown in Table I. The electron plasma density scale length is calculated by fitting the density profile along the axis to a function of the form $\exp(-x/l_s)$. It has been previously discussed by Tao *et al.*[8] that the additional energy loss due to lateral expansion for a smaller spot size can be offset by lower reabsorption of in-band EUV light by the surrounding plasma indicated by a shorter plasma scale length. The metrology LPP scale length is so much shorter than the HVM scale length that the CE actually increases.

Figure 2 shows the simulated electron density, temperature, and laser absorption profiles along the laser axis at the peak of the laser pulse for both spot sizes. Although the

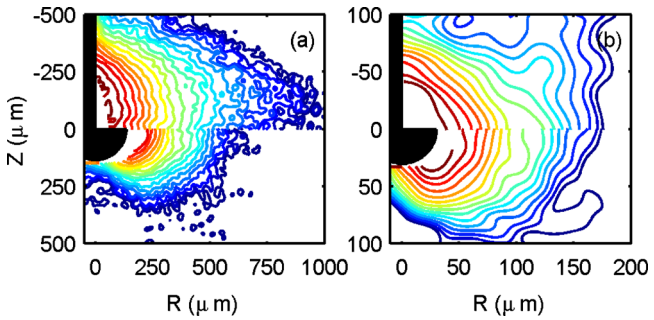

FIG. 1. (Color online) Contours of the plasma electron density at the peak of the laser pulse for planar (top) and spherical target (bottom) for (a) 150 and (b) 26 μm laser spot size plasma. The contour lines correspond to log 10 (n_e) values of (a) 19.4–17.6 and (b) 19.8–18.4 in 0.1 increments.

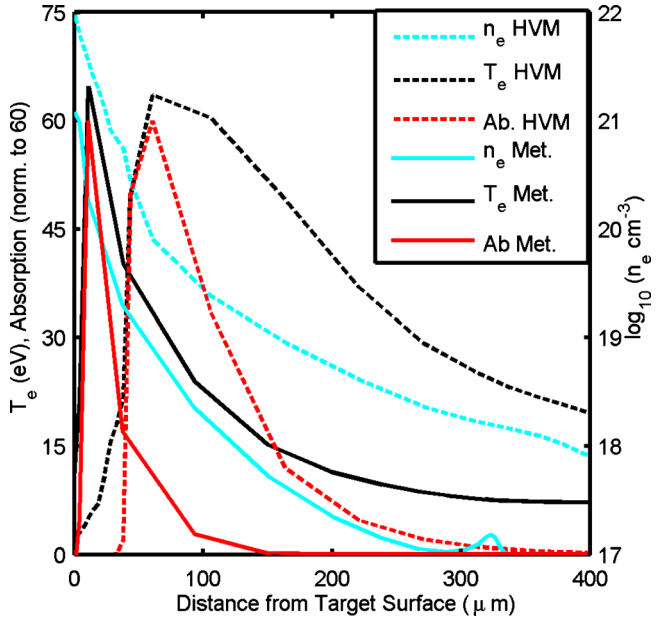

FIG. 2. (Color online) Simulations of the HVM (dashed lines) and metrology (solid lines) electron density (blue), electron temperature (black) and normalized laser absorption (red) along the laser axis at the peak of the laser pulse.

maximum plasma temperature is lower for the metrology plasma before the peak of the laser pulse, which will be discussed later, both plasmas reach a maximum electron temperature of approximately 65 eV at the peak of the laser pulse but with dramatically different plasma scale lengths. The one-dimensional (1D) plasma expansion equation $l_s = \sqrt{ZT_e/M_i}\tau_{Laser}$, where Z is the average charge state, T_e is the electron temperature, M_i is the ion mass, and τ_{Laser} is the laser pulse duration, is no longer valid for such a small spot size.[18] Additionally, Figs. 1(a) and 1(b) also show that the metrology plasma density is less affected by the target geometry. The larger focal spot size plasmas are closer to ideal 1D plasma expansion. The addition of spherical target geometry will increase the 2D expansion compared to planar targets. However, there is already more "natural" lateral expansion for the smaller metrology focal spot size. This makes the increase in 2D expansion due to target geometry have a less significant effect on plasma expansion and scale length, shown in Table I.

The electron density scale length has a significant effect on the electron densities at which the laser absorption takes place resulting in different power balance equation.[19] Figure 2 shows the laser penetrates deeper and to higher densities for the metrology LPP. As a result the absorption is narrower and occurs at higher densities for the metrology plasma with very little laser light reaching the critical density in either case. The difference in the electron densities that laser absorption occurs affects the EUV radiation transport and emission of the LPP.

Typical profiles of the time-resolved in-band EUV emission and laser pulse for both laser focal spots sizes are shown in Fig. 3. There are three notable differences in the metrology EUV emission: (1) 2 ns delay between the laser and the start of EUV emission, (2) shorter FWHM of EUV emission, and (3) the peak EUV emission occur later in time. The EUV delay is a combination of several factors. Simulations show that the metrology LPP does not heat as quickly as the HVM

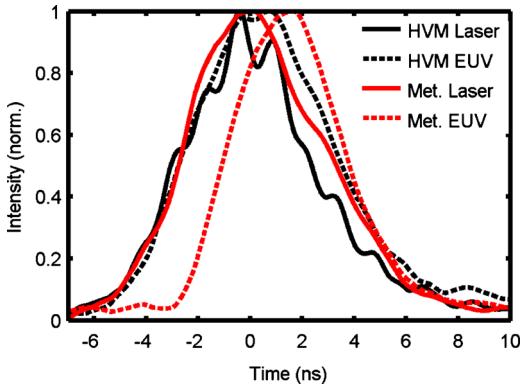

FIG. 3. (Color online) Normalized experimental time-resolved HVM laser pulse (solid black), HVM EUV emission (dashed black), metrology laser pulse (solid red), and metrology in-band EUV emission (dashed red).

LPP mainly from an increase in energy transported out of the core of the plasma due to lateral expansion. This is not contradictory to Fig. 2 (showing the same peak temperature at the peak of the laser pulse) as the narrower laser absorption region of the metrology LPP overcomes the early inefficient heating of the plasma. Also, less in-band EUV can escape from the absorption region of the metrology LPP due to higher opacity of the higher density region. Therefore, the combination of both the shorter plasma scale length and higher absorption density requires more time for the metrology LPP to expand and allow the optimum temperature to expand to a lower, more optically thin density that efficiently emit in-band EUV. The delay of in-band EUV emission results in shorter in-band EUV emission for the metrology LPP.

As previously discussed for Nd:YAG Sn LPP, the dense overheated core of the plasma contains additional energy that is transmitted to regions of lower densities after the peak of the laser pulse, thus allowing continued in-band EUV emission.[13] Here, the metrology plasma has a higher energy density core than the HVM plasma, both having the same electron temperature but the metrology plasma having higher electron densities. This allows longer continued EUV emission, resulting in the peak of the EUV emission occurring 0.8 ns later than HVM EUV emission peak.

Figures 4(a) and 4(b) shows typical time-integrated in-band EUV images for the metrology and HVM Sn LPPs, respectively, which are used to calculated the source brightness. Also plotted for comparison purposes in Fig. 4 are black lines corresponding to twice the diameter of the laser focal spot. The lines clearly show that the metrology dominant in-band EUV emitting region (DER) has more lateral expansion than that of the HVM plasma. A simplified equation derived by Banine and Moors[20] for a spherical emitting region for the source etendue is $E_{source}=(\pi/4)D^2\Omega_{col}$, where D is the source diameter and Ω_{col} is the collector solid angle (2π sr). While the DERs are not perfectly spherical, the equation will give a rough idea of the source brightness. Assuming state of the art droplet frequency of 50 kHz,[21] the HVM could output 162 W and the metrology 9 W. Operating at 50 kHz, the EUV brightness would be approximately 345 W mm^{-2} sr^{-1} and 380 W mm^{-2} sr^{-1} for the HVM and metrology LPP, respectively. Whereas the EUV emission is shorter for the metrology LPP, the shorter scale of the metrology LPP leads to less reabsorption of EUV by the surrounding plasma and ultimately a brighter EUV light source.

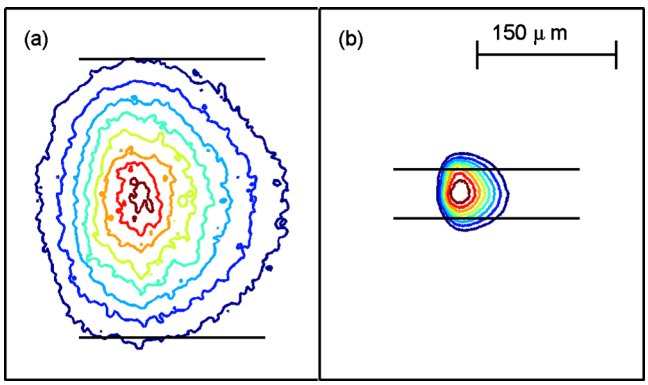

FIG. 4. (Color online) Normalized time-integrated EUV emission images for a Sn LPP with spot size of (a) 150 and (b) 26 μm. Also plotted are horizontal lines (black) corresponding to twice the width of the laser focal spot size.

The authors would like to acknowledge both General Atomics and Cascade Applied Sciences, Inc. for the use of and support with h2d. This work was supported by KLA-Tencor and by the University of California (UC) under the UC Industry-University Cooperative Research Program (ele128478) and by a gift from Cymer Inc.

[1]C. Wagner and N. Harned, Nat. Photonics **4**, 24 (2010).
[2]S. Bajt, J. Alameda, T. Barbee, Jr., W. Clift, J. Folta, B. Kaufmann, and E. Spiller, Opt. Eng. **41**, 1797 (2002).
[3]K. Goldberg, 2008 International Workshop on EUV Lithography, Wailea, Maui, Hawaii, 2008.
[4]P. Naulleau, K. Goldberg, S. Lee, C. Chang, D. Attwood, and J. Bokor, Appl. Opt. **38**, 7252 (1999).
[5]R. Klein, C. Laubis, R. Müller, F. Scholze, and G. Ulm, Microelectron. Eng. **83**, 707 (2006).
[6]I. Fomenkov, D. Brandt, A. Bykanov, A. Ershov, W. Partlo, D. Myers, N. Böwering, G. Vaschenko, O. Khodykin, and J. Hoffman, Proc. SPIE **6517**, 65173J (2007).
[7]Y. Tao, M. S. Tillack, K. L. Sequoia, R. A. Burdt, S. Yuspeh, and F. Najmabadi, Appl. Phys. Lett. **92**, 251501 (2008).
[8]Y. Tao, S. S. Harilal, M. S. Tillack, K. L. Sequoia, B. O'Shay, and F. Najmabadi, Opt. Lett. **31**, 2492 (2006).
[9]S. S. Harilal, R. W. Coons, P. Hough, and A. Hassanein, Appl. Phys. Lett. **95**, 221501 (2009).
[10]K. Hou, S. George, A. Mordovanakis, K. Takenoshita, J. Nees, B. Lafontaine, M. Richardson, and A. Galvanauskas, Opt. Express **16**, 965 (2008).
[11]A. Bayer, F. Barkusky, S. D^ring, P. Groflmann, and K. Mann, X-Ray Optics and Instrumentation, 687496 (2010).
[12]I. Turcu and J. Dance, *X-rays from Laser Plasmas: Generation and Applications* (Wiley, New York, 1998).
[13]S. Yuspeh, K. L. Sequoia, Y. Tao, M. S. Tillack, R. A. Burdt, and F. Najmabadi, Appl. Phys. Lett. **96**, 261501 (2010).
[14]S. Yuspeh, K. L. Sequoia, Y. Tao, M. S. Tillack, R. Burdt, and F. Najmabadi, Appl. Phys. Lett. **93**, 221503 (2008).
[15]K. L. Sequoia, Y. Tao, S. Yuspeh, R. Burdt, and M. S. Tillack, Appl. Phys. Lett. **92**, 221505 (2008).
[16]J. Larson, h2d is a commercial product of Cascade Applied Sciences Incorporated, 6325 Trevarton Drive, Longmont, CO 80503. Electronic mail: larsen@casinc.com.
[17]S. Fujioka, H. Nishimura, K. Nishihara, A. Sasaki, A. Sunahara, T. Okuno, N. Ueda, T. Ando, Y. Tao, and Y. Shimada, Phys. Rev. Lett. **95**, 235004 (2005).
[18]W. Kruer, *The Physics of Laser Plasma Interactions* (Westview, Boulder, 2003).
[19]K. Nishihara, A. Sunahara, A. Sasaki, M. Nunami, H. Tanuma, S. Fujioka, Y. Shimada, K. Fujima, H. Furukawa, and T. Kato, Phys. Plasmas **15**, 056708 (2008).
[20]V. Banine and R. Moors, J. Phys. D: Appl. Phys **37**, 3207 (2004).
[21]D. Brandt, I. Fomenkov, A. Ershov, W. Partlo, D. Myers, N. Böwering, N. Farrar, G. Vaschenko, O. Khodykin, and A. Bykanov, Proc. SPIE **7271**, 727103 (2009).